

SIMULATION OF LINEAR COUPLING RESONANCE TRAVERSAL IN THE AGS BOOSTER

C. J. Gardner

November 1993

Collider Accelerator Department
Brookhaven National Laboratory

U.S. Department of Energy

USDOE Office of Science (SC)

Notice: This technical note has been authored by employees of Brookhaven Science Associates, LLC under Contract No. DE-AC02-76CH00016 with the U.S. Department of Energy. The publisher by accepting the technical note for publication acknowledges that the United States Government retains a non-exclusive, paid-up, irrevocable, world-wide license to publish or reproduce the published form of this technical note, or allow others to do so, for United States Government purposes.

DISCLAIMER

This report was prepared as an account of work sponsored by an agency of the United States Government. Neither the United States Government nor any agency thereof, nor any of their employees, nor any of their contractors, subcontractors, or their employees, makes any warranty, express or implied, or assumes any legal liability or responsibility for the accuracy, completeness, or any third party's use or the results of such use of any information, apparatus, product, or process disclosed, or represents that its use would not infringe privately owned rights. Reference herein to any specific commercial product, process, or service by trade name, trademark, manufacturer, or otherwise, does not necessarily constitute or imply its endorsement, recommendation, or favoring by the United States Government or any agency thereof or its contractors or subcontractors. The views and opinions of authors expressed herein do not necessarily state or reflect those of the United States Government or any agency thereof.

Accelerator Division
Alternating Gradient Synchrotron Department
BROOKHAVEN NATIONAL LABORATORY
Upton, New York 11973

Accelerator Division
Technical Note

AGS/AD/Tech. Note No. 385

**SIMULATION OF LINEAR COUPLING RESONANCE
TRAVERSAL IN THE AGS BOOSTER**

C.J. Gardner

November 8, 1993

Simulation of Linear Coupling Resonance Traversal in the AGS Booster

C. J. Gardner

November 8, 1993

1 Introduction

The exchange of the horizontal and vertical emittances upon traversal of the linear coupling resonance was observed some years ago in the AGS during the acceleration of polarized protons and has been observed more recently during studies in the AGS Booster. Here we develop a simple simulation of the coupling resonance traversal and demonstrate the effect on the emittances.

2 Formulae for the Evolution of a Gaussian Beam Distribution

We assume that the initial beam distribution is gaussian and is given by

$$\rho_0(\mathbf{Z}_0) = \left(\frac{1}{2\pi\epsilon}\right)^2 e^{-W_0}, \quad W_0 = \frac{1}{2\epsilon} \mathbf{Z}_0^\dagger \mathbf{E}_0^{-1} \mathbf{Z}_0, \quad \mathbf{Z}_0 = \begin{pmatrix} x_0 \\ x'_0 \\ y_0 \\ y'_0 \end{pmatrix}, \quad (1)$$

where x_0, x'_0, y_0, y'_0 are the horizontal and vertical positions and angles of a beam particle with respect to the reference trajectory at a point s_0 along the trajectory, and \mathbf{E}_0 is a four-by-four real, symmetric, positive definite matrix with unit determinant. Then, as shown in the Appendix, the beam distribution at a subsequent point s along the trajectory is also gaussian

and is given by

$$\rho(\mathbf{Z}) = \left(\frac{1}{2\pi\epsilon} \right)^2 e^{-W}, \quad W = \frac{1}{2\epsilon} \mathbf{Z}^\dagger \mathbf{E}^{-1} \mathbf{Z}, \quad \mathbf{Z} = \begin{pmatrix} x \\ x' \\ y \\ y' \end{pmatrix}, \quad (2)$$

where

$$\mathbf{E} = \mathbf{T} \mathbf{E}_0 \mathbf{T}^\dagger, \quad (3)$$

\mathbf{T} is the symplectic four-by-four transfer matrix between s_0 and s , and \mathbf{E} is real, symmetric, positive definite, and has unit determinant. Equations (2) and (3) give the evolution of the gaussian beam distribution as it moves along a beam line or around a ring.

The projections of the distribution (2) on the x, x' and y, y' planes are

$$P_1(x, x') = \int \rho(\mathbf{Z}) dy dy', \quad P_2(y, y') = \int \rho(\mathbf{Z}) dx dx', \quad (4)$$

and doing the integration (see Appendix) one finds

$$P_1(x, x') = \frac{1}{2\pi e_1} e^{-W_1}, \quad W_1 = \frac{1}{2e_1} (g_1 x^2 + 2a_1 x x' + b_1 x'^2), \quad (5)$$

$$P_2(y, y') = \frac{1}{2\pi e_2} e^{-W_2}, \quad W_2 = \frac{1}{2e_2} (g_2 y^2 + 2a_2 y y' + b_2 y'^2), \quad (6)$$

where

$$e_1 = \epsilon (E_{11} E_{22} - E_{12}^2)^{1/2} = \epsilon D_1, \quad e_2 = \epsilon (E_{33} E_{44} - E_{34}^2)^{1/2} = \epsilon D_2, \quad (7)$$

$$a_1 = -E_{12}/D_1, \quad b_1 = E_{11}/D_1, \quad g_1 = E_{22}/D_1, \quad (8)$$

$$a_2 = -E_{34}/D_2, \quad b_2 = E_{33}/D_2, \quad g_2 = E_{44}/D_2. \quad (9)$$

The projections are therefore gaussian distributions with rms emittances e_1 and e_2 . The evolution of the projection parameters is obtained by substituting the matrix elements, E_{ij} , obtained from (3) into equations (7-9).

3 Simulation Algorithm

To produce linear coupling in the booster we perturb the lattice with six thin skew quadrupoles equally spaced (one per superperiod) around the ring. The transfer matrix for each thin skew quad is (see Appendix)

$$\mathbf{q} = \begin{pmatrix} \mathbf{I} & \mathbf{k} \\ \mathbf{k} & \mathbf{I} \end{pmatrix}, \quad \mathbf{k} = \begin{pmatrix} 0 & 0 \\ k & 0 \end{pmatrix}, \quad (10)$$

where k is the integrated strength. The transfer matrix for one superperiod of the unperturbed lattice is,

$$\mathbf{t} = \begin{pmatrix} \mathbf{M} & \mathbf{0} \\ \mathbf{0} & \mathbf{N} \end{pmatrix}, \quad (11)$$

where

$$\mathbf{M} = \mathbf{I} \cos \psi_x + \mathbf{J}_x \sin \psi_x, \quad \mathbf{J}_x = \begin{pmatrix} \alpha_x & \beta_x \\ -\gamma_x & -\alpha_x \end{pmatrix}, \quad (12)$$

$$\mathbf{N} = \mathbf{I} \cos \psi_y + \mathbf{J}_y \sin \psi_y, \quad \mathbf{J}_y = \begin{pmatrix} \alpha_y & \beta_y \\ -\gamma_y & -\alpha_y \end{pmatrix}, \quad (13)$$

$$\mathbf{I} = \begin{pmatrix} 1 & 0 \\ 0 & 1 \end{pmatrix}, \quad \psi_x = 2\pi Q_x/6, \quad \psi_y = 2\pi Q_y/6, \quad (14)$$

Q_x and Q_y are the horizontal and vertical tunes, and $\alpha_x, \beta_x, \gamma_x, \alpha_y, \beta_y, \gamma_y$ are the Courant-Snyder parameters at the location of each skew quad. The complete one-turn transfer matrix through six superperiods is then

$$\mathbf{T} = (\mathbf{tq})^6. \quad (15)$$

To simulate the traversal of the linear coupling resonance we calculate the turn-by-turn evolution of the gaussian distribution as the tunes pass through the resonance $Q_x - Q_y = 0$. Let Q_{xn}, Q_{yn}, k_n be the tunes and skew quad strength on the n th turn around the machine. Then the one-turn transfer matrix, \mathbf{T}_n , on the n th turn is obtained by substituting these values into equations (10–15), and it follows from (3) that

$$\mathbf{E}_{n+1} = \mathbf{T}_n \mathbf{E}_n \mathbf{T}_n^\dagger, \quad (16)$$

where \mathbf{E}_n and \mathbf{E}_{n+1} are the matrices which define the gaussian beam distribution on the n th and $(n+1)$ th turns. The turn-by-turn evolution of

the gaussian distribution and it's projections can then be obtained quite simply with computer code which, when supplied with the one-turn transfer matrix \mathbf{T}_n and the initial matrix \mathbf{E}_0 , calculates \mathbf{E}_n after each turn using the recursion relation (16).

4 Results

We shall assume that the initial beam distribution is the product of two gaussian distributions, ρ_x and ρ_y , which are matched to the unperturbed lattice at the location of the skew quads. Thus we have

$$\rho_0(\mathbf{Z}_0) = \rho_x(x_0, x'_0) \rho_y(y_0, y'_0), \quad (17)$$

where

$$\rho_x(x, x') = \frac{1}{2\pi\epsilon_x} e^{-W_x}, \quad W_x = \frac{1}{2\epsilon_x} (\gamma_x x^2 + 2\alpha_x x x' + \beta_x x'^2), \quad (18)$$

$$\rho_y(y, y') = \frac{1}{2\pi\epsilon_y} e^{-W_y}, \quad W_y = \frac{1}{2\epsilon_y} (\gamma_y y^2 + 2\alpha_y y y' + \beta_y y'^2), \quad (19)$$

ϵ_x and ϵ_y are the initial rms emittances, and $\alpha_x, \beta_x, \gamma_x, \alpha_y, \beta_y, \gamma_y$ are the unperturbed lattice parameters at the location of the skew quad in each superperiod. The values of these parameters obtained from the MAD code are $\alpha_x = -1.60, \beta_x = 11.34, \alpha_y = 0.76, \beta_y = 4.76$.

Comparing equations (17–19) with (1) we obtain the initial matrix, \mathbf{E}_0 , to be used in the recursion relation (16);

$$\mathbf{E}_0^{-1} = \begin{pmatrix} \epsilon \mathbf{A}_x^{-1} / \epsilon_x & \mathbf{0} \\ \mathbf{0} & \epsilon \mathbf{A}_y^{-1} / \epsilon_y \end{pmatrix}, \quad \epsilon = \sqrt{\epsilon_x \epsilon_y} \quad (20)$$

where

$$\mathbf{A}_x^{-1} = \begin{pmatrix} \gamma_x & \alpha_x \\ \alpha_x & \beta_x \end{pmatrix}, \quad \mathbf{A}_y^{-1} = \begin{pmatrix} \gamma_y & \alpha_y \\ \alpha_y & \beta_y \end{pmatrix}. \quad (21)$$

4.1 Adiabatic Traversal of Resonance

We consider first the case for which the tunes and skew quad strength on the n th turn are given by

$$Q_{xn} = Q_{x0} + n \delta Q_x, \quad Q_{yn} = Q_{y0} + n \delta Q_y, \quad k_n = (N - |N - n|) \delta k, \quad (22)$$

where

$$Q_{x0} = 8.80, \quad \delta Q_x = 0.01/1000, \quad Q_{y0} = 8.82, \quad \delta Q_y = 0, \quad (23)$$

$$\delta k = \frac{KI}{Np}, \quad K = (.000545/3.335641) \text{ m}^{-1}/\text{amp}, \quad N = 2000, \quad (24)$$

I is the skew quad current in Amps, and p is the momentum in GeV/c. Thus the vertical tune is fixed at 4.82, while the horizontal tune increases linearly from 4.80 to 4.84 over 4000 turns, crossing the $Q_x - Q_y = 0$ resonance on the 2000th turn. The skew quad strength increases linearly from 0 to KI/p over the first 2000 turns and then decreases linearly to 0 over the next 2000 turns. Choosing initial emittances $\epsilon_x = 0.7$, $\epsilon_y = 0.3$, and $I/p = 2.0$ we obtain the projection emittances, e_1 and e_2 , shown versus turn in Figure 1. Here we see that the horizontal and vertical emittances are exchanged during the resonance traversal. Figure 2 is a plot of $e_1 + e_2 - (\epsilon_x + \epsilon_y) = e_1 + e_2 - 1$ which shows that the sum of the projection emittances differs from the sum of the initial emittances by only a very small amount during the resonance traversal and returns to the initial sum at the end of the 4000 turns. The plot also shows that the sum of the projection emittances is always greater than or equal to the sum of the initial uncoupled emittances, a result which Brown and Servranckx [2] have shown to be true under quite general conditions (see Appendix). Figures 3 and 4 are plots of $(a_1 - \alpha_x)/\alpha_x$, $(b_1 - \beta_x)/\beta_x$ and $(a_2 - \alpha_y)/\alpha_y$, $(b_2 - \beta_y)/\beta_y$ which show that the ellipse parameters of the x , x' and y , y' projections differ from the unperturbed lattice parameters by only very small amounts during the resonance traversal and return to their initial values at the end of the 4000 turns. This is the behavior expected for an adiabatic traversal of the resonance. Figures (5–8) and (9–12) are the corresponding plots for the cases in which $I/p = 0.2$ and $I/p = 20$.

For the case in which the skew quad strength is held constant during the 4000 turns, i.e. $k_n = KI/p = 2.0K$ in equation (22), we obtain the plots shown in Figures (13–16). Here we see that $e_1 + e_2 - 1$ is very small as before but continues to oscillate rather than settling down to zero after passing through the resonance. The same is true of $(a_1 - \alpha_x)/\alpha_x$, $(b_1 - \beta_x)/\beta_x$, $(a_2 - \alpha_y)/\alpha_y$, and $(b_2 - \beta_y)/\beta_y$.

4.2 Nonadiabatic Traversal of Resonance

Now consider the case for which the tunes and skew quad strength on the n th turn are given by (22), but the skew quads are ‘snapped’ OFF on the 2000th turn and stay off for the remaining turns. (The skew quad strength increases linearly from 0 to KI/p over the first 2000 turns.) The resulting projection parameters for the case in which $I/p = 2.0$ are shown versus turn in Figures (17–20). Here we see that the projection parameters $(a_1 - \alpha_x)/\alpha_x$, $(b_1 - \beta_x)/\beta_x$, $(a_2 - \alpha_y)/\alpha_y$, $(b_2 - \beta_y)/\beta_y$, and $e_1 + e_2 - 1$ are small as before but continue to oscillate after passing through the resonance.

For the case in which the skew quad current is ‘snapped’ ON with $I/p = 2.0$ at 2000 turns and then decreases linearly to 0 over the next 2000 turns we obtain the projection parameters versus turn shown in Figures (21–24). Here we see that $e_1 + e_2 - 1$ settles down to zero, but the other projection parameters continue to oscillate after passing through the resonance.

5 Appendix

5.1 Transport of the Beam Ellipsoid

Let x_0, x'_0, y_0, y'_0 be the horizontal and vertical positions and angles of a beam particle with respect to the reference trajectory at a point s_0 along the trajectory. Then the positions, x and y , and angles, x' and y' , of the particle at the point s along the trajectory are given by

$$\mathbf{Z} = \mathbf{T}\mathbf{Z}_0, \quad (25)$$

where

$$\mathbf{Z} = \begin{pmatrix} x \\ x' \\ y \\ y' \end{pmatrix}, \quad \mathbf{Z}_0 = \begin{pmatrix} x_0 \\ x'_0 \\ y_0 \\ y'_0 \end{pmatrix} \quad (26)$$

and \mathbf{T} is the four-by-four transfer matrix between s_0 and s . The matrix \mathbf{T} is symplectic:

$$\mathbf{T}^\dagger \mathbf{S} \mathbf{T} = \mathbf{S}, \quad |\mathbf{T}| = 1, \quad (27)$$

where

$$\mathbf{S} = \begin{pmatrix} 0 & 1 & 0 & 0 \\ -1 & 0 & 0 & 0 \\ 0 & 0 & 0 & 1 \\ 0 & 0 & -1 & 0 \end{pmatrix}, \quad \mathbf{S}^2 = -\mathbf{I} = \begin{pmatrix} -1 & 0 & 0 & 0 \\ 0 & -1 & 0 & 0 \\ 0 & 0 & -1 & 0 \\ 0 & 0 & 0 & -1 \end{pmatrix}, \quad (28)$$

and a \dagger denotes the transpose of the matrix.

Suppose the beam at s_0 is contained within the ellipsoid defined by

$$\mathbf{Z}_0^\dagger \mathbf{E}_0^{-1} \mathbf{Z}_0 = \epsilon \quad (29)$$

where \mathbf{E}_0 is a four-by-four real, symmetric, positive definite matrix with unit determinant. Then it is easy to show that the ellipsoid at s_0 is transformed into another ellipsoid at s . Using (25) in (29) we find

$$\mathbf{Z}^\dagger \mathbf{E}^{-1} \mathbf{Z} = \epsilon, \quad (30)$$

where

$$\mathbf{E} = \mathbf{T} \mathbf{E}_0 \mathbf{T}^\dagger. \quad (31)$$

Equation (30) defines an ellipsoid provided the matrix \mathbf{E}^{-1} is symmetric and positive definite. Using (31) and (27) we find

$$\mathbf{E}^\dagger = \mathbf{T} \mathbf{E}_0^\dagger \mathbf{T}^\dagger = \mathbf{T} \mathbf{E}_0 \mathbf{T}^\dagger = \mathbf{E}, \quad |\mathbf{E}| = |\mathbf{T}| |\mathbf{E}_0| |\mathbf{T}^\dagger| = 1. \quad (32)$$

Thus, \mathbf{E} and \mathbf{E}^{-1} are symmetric and have unit determinant. Now a real and symmetric matrix, \mathbf{A} , is positive definite if the quadratic form $\mathbf{Z}^\dagger \mathbf{A} \mathbf{Z} > 0$ for every $\mathbf{Z} \neq \mathbf{0}$. To show that \mathbf{E}^{-1} is positive definite, consider

$$\mathbf{Z}^\dagger \mathbf{E}^{-1} \mathbf{Z} = \mathbf{Z}_0^\dagger \mathbf{T}^\dagger \mathbf{E}^{-1} \mathbf{T} \mathbf{Z}_0 = \mathbf{Z}_0^\dagger \mathbf{E}_0^{-1} \mathbf{Z}_0. \quad (33)$$

Since $\mathbf{Z}_0^\dagger \mathbf{E}_0^{-1} \mathbf{Z}_0 > 0$ for all $\mathbf{Z}_0 \neq \mathbf{0}$, and since $\mathbf{Z} = \mathbf{0}$ if and only if $\mathbf{Z}_0 = \mathbf{0}$, it follows that $\mathbf{Z}^\dagger \mathbf{E}^{-1} \mathbf{Z} > 0$ for all $\mathbf{Z} \neq \mathbf{0}$. Therefore \mathbf{E}^{-1} is positive definite, and the ellipsoid defined by \mathbf{E}_0 is transformed into another ellipsoid defined by \mathbf{E} in going from s_0 to s . The phase space volume enclosed by the ellipsoid is conserved and any particle inside (outside) the ellipsoid at s_0 will also be inside (outside) the ellipsoid at s .

5.2 Transport of Gaussian Beam Distribution

Suppose the beam density at \mathbf{Z}_0 is given by the gaussian distribution

$$\rho_0(\mathbf{Z}_0) = \left(\frac{1}{2\pi\epsilon} \right)^2 e^{-W_0}, \quad W_0 = \frac{1}{2\epsilon} \mathbf{Z}_0^\dagger \mathbf{E}_0^{-1} \mathbf{Z}_0. \quad (34)$$

Then according to Liouville's Theorem the beam density, $\rho(\mathbf{Z})$, at $\mathbf{Z} = \mathbf{T}\mathbf{Z}_0$ is just $\rho_0(\mathbf{Z}_0)$, and it follows from (25) and (34) that

$$\rho(\mathbf{Z}) = \left(\frac{1}{2\pi\epsilon} \right)^2 e^{-W}, \quad W = \frac{1}{2\epsilon} \mathbf{Z}^\dagger \mathbf{E}^{-1} \mathbf{Z}, \quad (35)$$

where $\mathbf{E} = \mathbf{T}\mathbf{E}_0\mathbf{T}^\dagger$. These equations give the evolution of a gaussian beam distribution as it moves along a beam line or around a ring.

5.3 Second Moments of Gaussian Distribution

The second moments,

$$\langle Z_i Z_j \rangle = \int Z_i Z_j \rho(\mathbf{Z}) d^4 Z, \quad (36)$$

of the distribution can be calculated by transforming to a representation in which \mathbf{E}^{-1} is diagonal. Since \mathbf{E} is real and symmetric there exists an orthogonal matrix, \mathbf{O} , which diagonalizes \mathbf{E} . Thus we have

$$\mathbf{O}\mathbf{E}\mathbf{O}^\dagger = \mathbf{e}, \quad e_{ij} = e_i \delta_{ij}, \quad \mathbf{O}\mathbf{O}^\dagger = \mathbf{I}, \quad (37)$$

and defining $\mathbf{Y} = \mathbf{O}\mathbf{Z}$, equation (36) becomes

$$\langle Z_i Z_j \rangle = \sum_{kl} \int O_{ik}^\dagger Y_k O_{jl}^\dagger Y_l \rho(\mathbf{Y}) |\mathbf{O}^\dagger| d^4 Y, \quad (38)$$

where

$$\rho(\mathbf{Y}) = \left(\frac{1}{2\pi\epsilon} \right)^2 e^{-W}, \quad W = \frac{1}{2\epsilon} \mathbf{Y}^\dagger \mathbf{e}^{-1} \mathbf{Y}. \quad (39)$$

Thus

$$\langle Z_i Z_j \rangle = \sum_{kl} O_{ik}^\dagger \langle Y_k Y_l \rangle O_{lj}, \quad \langle Y_k Y_l \rangle = \int Y_k Y_l \rho(\mathbf{Y}) d^4 Y. \quad (40)$$

Applying the integrals

$$\int_{-\infty}^{+\infty} e^{-A^2 Y^2} dY = \frac{\sqrt{\pi}}{A}, \quad \int_{-\infty}^{+\infty} Y^2 e^{-A^2 Y^2} dY = \frac{\sqrt{\pi}}{2A^3}, \quad (41)$$

and using $|\mathbf{e}| = 1$ we find

$$\langle Y_k Y_l \rangle = \epsilon e_k \delta_{kl} \quad (42)$$

and therefore

$$\langle Z_i Z_j \rangle = \epsilon \sum_{kl} O_{ik}^\dagger e_{kl} O_{lj} = \epsilon E_{ij}. \quad (43)$$

5.4 Projections

It is useful to partition the matrices in equations (25) and (31) into two-by-two matrices. Introducing the notation

$$\mathbf{E}_0 = \begin{pmatrix} \mathbf{F}_0 & \mathbf{C}_0 \\ \mathbf{C}_0^\dagger & \mathbf{G}_0 \end{pmatrix}, \quad \mathbf{E} = \begin{pmatrix} \mathbf{F} & \mathbf{C} \\ \mathbf{C}^\dagger & \mathbf{G} \end{pmatrix}, \quad \mathbf{T} = \begin{pmatrix} \mathbf{M} & \mathbf{n} \\ \mathbf{m} & \mathbf{N} \end{pmatrix} \quad (44)$$

and

$$\mathbf{U}_0 = \begin{pmatrix} x_0 \\ x'_0 \end{pmatrix}, \quad \mathbf{V}_0 = \begin{pmatrix} y_0 \\ y'_0 \end{pmatrix}, \quad \mathbf{U} = \begin{pmatrix} x \\ x' \end{pmatrix}, \quad \mathbf{V} = \begin{pmatrix} y \\ y' \end{pmatrix} \quad (45)$$

where $\mathbf{F}_0, \mathbf{G}_0, \mathbf{C}_0, \mathbf{F}, \mathbf{G}, \mathbf{C}, \mathbf{M}, \mathbf{N}, \mathbf{m}, \mathbf{n}$ are two-by-two matrices, the equation $\mathbf{E} = \mathbf{T}\mathbf{E}_0\mathbf{T}^\dagger$ becomes

$$\mathbf{F} = \mathbf{M}\mathbf{F}_0\mathbf{M}^\dagger + \mathbf{n}\mathbf{G}_0\mathbf{n}^\dagger + \mathbf{n}\mathbf{C}_0^\dagger\mathbf{M}^\dagger + \mathbf{M}\mathbf{C}_0\mathbf{n}^\dagger, \quad (46)$$

$$\mathbf{G} = \mathbf{N}\mathbf{G}_0\mathbf{N}^\dagger + \mathbf{m}\mathbf{F}_0\mathbf{m}^\dagger + \mathbf{N}\mathbf{C}_0^\dagger\mathbf{m}^\dagger + \mathbf{m}\mathbf{C}_0\mathbf{N}^\dagger, \quad (47)$$

$$\mathbf{C} = \mathbf{M}\mathbf{C}_0\mathbf{N}^\dagger + \mathbf{n}\mathbf{C}_0^\dagger\mathbf{m}^\dagger + \mathbf{M}\mathbf{F}_0\mathbf{m}^\dagger + \mathbf{n}\mathbf{G}_0\mathbf{N}^\dagger, \quad (48)$$

and $\mathbf{Z} = \mathbf{T}\mathbf{Z}_0$ becomes

$$\mathbf{U} = \mathbf{M}\mathbf{U}_0 + \mathbf{n}\mathbf{V}_0, \quad \mathbf{V} = \mathbf{m}\mathbf{U}_0 + \mathbf{N}\mathbf{V}_0. \quad (49)$$

Here we see that if the initial ellipsoid defined by \mathbf{E}_0 has no correlation between the x and y planes, then $\mathbf{C}_0 = \mathbf{0}$ and equations (46–48) become

$$\mathbf{F} = \mathbf{M}\mathbf{F}_0\mathbf{M}^\dagger + \mathbf{n}\mathbf{G}_0\mathbf{n}^\dagger, \quad (50)$$

$$\mathbf{G} = \mathbf{N}\mathbf{G}_0\mathbf{N}^\dagger + \mathbf{m}\mathbf{F}_0\mathbf{m}^\dagger, \quad (51)$$

$$\mathbf{C} = \mathbf{M}\mathbf{F}_0\mathbf{m}^\dagger + \mathbf{n}\mathbf{G}_0\mathbf{N}^\dagger. \quad (52)$$

On the other hand, if there is no coupling in the transfer matrix, \mathbf{T} , then $\mathbf{m} = \mathbf{n} = \mathbf{0}$ and we have

$$\mathbf{F} = \mathbf{M}\mathbf{F}_0\mathbf{M}^\dagger, \quad \mathbf{G} = \mathbf{N}\mathbf{G}_0\mathbf{N}^\dagger, \quad \mathbf{C} = \mathbf{M}\mathbf{C}_0\mathbf{N}^\dagger. \quad (53)$$

5.4.1 Projections of the Beam Ellipsoid

Consider the ellipsoid $\mathbf{Z}_0^\dagger \mathbf{E}_0^{-1} \mathbf{Z}_0 = \epsilon$. We wish to find the equations for the boundaries of the projections of this ellipsoid onto the x_0, x'_0 and y_0, y'_0 planes. To find the projection on the x_0, x'_0 plane we seek a transformation, \mathbf{T} , from coordinates $\mathbf{U}_0, \mathbf{V}_0$ to new coordinates \mathbf{U}, \mathbf{V} such that $\mathbf{U} = \mathbf{U}_0$ and the equation for the transformed ellipsoid is of the form

$$\mathbf{U}^\dagger \mathbf{F}^{-1} \mathbf{U} + \mathbf{V}^\dagger \mathbf{G}^{-1} \mathbf{V} = \epsilon, \quad (54)$$

where \mathbf{F}^{-1} and \mathbf{G}^{-1} are positive definite. We obtain such a transformation if we choose

$$\mathbf{M} = \mathbf{I}, \quad \mathbf{n} = \mathbf{0}, \quad \mathbf{m} = -\mathbf{N}\mathbf{C}_0^\dagger \mathbf{F}_0^{-1}, \quad |\mathbf{N}| = 1 \quad (55)$$

in the last of equations (44). Then the equation $\mathbf{E} = \mathbf{T}\mathbf{E}_0\mathbf{T}^\dagger$ becomes

$$\mathbf{F} = \mathbf{F}_0, \quad \mathbf{C} = \mathbf{0}, \quad \mathbf{G} = \mathbf{N}(\mathbf{G}_0 - \mathbf{C}_0^\dagger \mathbf{F}_0^{-1} \mathbf{C}_0)\mathbf{N}^\dagger, \quad (56)$$

and

$$\mathbf{U} = \mathbf{U}_0, \quad \mathbf{V} = \mathbf{N}(\mathbf{V}_0 - \mathbf{C}_0^\dagger \mathbf{F}_0^{-1} \mathbf{U}_0). \quad (57)$$

Thus

$$\mathbf{E}^{-1} = \begin{pmatrix} \mathbf{F}^{-1} & \mathbf{0} \\ \mathbf{0} & \mathbf{G}^{-1} \end{pmatrix}, \quad (58)$$

and the equation for the transformed ellipsoid is

$$\mathbf{U}^\dagger \mathbf{F}^{-1} \mathbf{U} + \mathbf{V}^\dagger \mathbf{G}^{-1} \mathbf{V} = \mathbf{U}_0^\dagger \mathbf{F}_0^{-1} \mathbf{U}_0 + \mathbf{V}^\dagger \mathbf{G}^{-1} \mathbf{V} = \epsilon. \quad (59)$$

Now since \mathbf{E}_0^{-1} is positive definite and since \mathbf{T}^{-1} exists, the matrix \mathbf{E}^{-1} is positive definite. The quadratic forms $\mathbf{U}_0^\dagger \mathbf{F}_0^{-1} \mathbf{U}_0$ and $\mathbf{V}^\dagger \mathbf{G}^{-1} \mathbf{V}$ are therefore positive definite and it follows that

$$\mathbf{U}_0^\dagger \mathbf{F}_0^{-1} \mathbf{U}_0 \leq \epsilon. \quad (60)$$

Defining

$$\mathbf{f}_0 = \mathbf{F}_0/D, \quad D = |\mathbf{F}_0|^{1/2} \quad (61)$$

we obtain

$$\mathbf{U}_0^\dagger \mathbf{f}_0^{-1} \mathbf{U}_0 \leq \epsilon D, \quad |\mathbf{f}_0| = 1 \quad (62)$$

which defines an elliptical region of area $\pi \epsilon D$. This region is the projection of the ellipsoid $\mathbf{Z}_0^\dagger \mathbf{E}_0^{-1} \mathbf{Z}_0 = \epsilon$ onto the x_0, x'_0 plane. The boundry of this region is given by

$$\mathbf{U}_0^\dagger \mathbf{F}_0^{-1} \mathbf{U}_0 = \epsilon, \quad (63)$$

and for these points we have

$$\mathbf{V}^\dagger \mathbf{G}^{-1} \mathbf{V} = 0, \quad \mathbf{V} = \mathbf{0}. \quad (64)$$

It follows from (57) and (64) that

$$\mathbf{V}_0 = \mathbf{C}_0^\dagger \mathbf{F}_0^{-1} \mathbf{U}_0. \quad (65)$$

These equations give the points on the surface of the ellipsoid which project onto the boundry of the x_0, x'_0 projection.

Generalizing the argument given above we find that the projection of the ellipsoid, $\mathbf{Z}^\dagger \mathbf{E}^{-1} \mathbf{Z} = \epsilon$, on the Z_m, Z_n plane is the elliptical region

$$\mathbf{U}^\dagger \mathbf{f}^{-1} \mathbf{U} \leq \epsilon D, \quad (66)$$

where

$$\mathbf{U} = \begin{pmatrix} Z_m \\ Z_n \end{pmatrix}, \quad D = (E_{mm}E_{nn} - E_{mn}^2)^{1/2}, \quad (67)$$

and the matrix elements of \mathbf{f} are

$$f_{11} = E_{mm}/D, \quad f_{22} = E_{nn}/D, \quad f_{12} = f_{21} = E_{mn}/D. \quad (68)$$

5.4.2 Projections of the Gaussian distribution

The projections of the gaussian distribution (35) on the x, x' and y, y' planes are

$$P_1(x, x') = \int \rho(\mathbf{Z}) dy dy', \quad P_2(y, y') = \int \rho(\mathbf{Z}) dx dx'. \quad (69)$$

Applying the integral

$$\int_{-\infty}^{+\infty} e^{-A^2 Z^2 \pm BZ} dZ = \frac{\sqrt{\pi}}{A} e^{B^2/(4A^2)} \quad (70)$$

we find that the projections are of the form

$$P_1(x, x') = \frac{1}{2\pi e_1} e^{-\lambda_1}, \quad \lambda_1 = (g_1 x^2 + 2a_1 x x' + b_1 x'^2)/2e_1, \quad (71)$$

$$P_2(y, y') = \frac{1}{2\pi e_2} e^{-\lambda_2}, \quad \lambda_2 = (g_2 y^2 + 2a_2 y y' + b_2 y'^2)/2e_2, \quad (72)$$

where

$$b_1 g_1 - a_1^2 = 1, \quad b_2 g_2 - a_2^2 = 1. \quad (73)$$

The second moments of the projections are then

$$\langle x^2 \rangle = e_1 b_1, \quad \langle x'^2 \rangle = e_1 g_1, \quad \langle x x' \rangle = -e_1 a_1, \quad (74)$$

$$\langle y^2 \rangle = e_2 b_2, \quad \langle y'^2 \rangle = e_2 g_2, \quad \langle y y' \rangle = -e_2 a_2. \quad (75)$$

These are, of course, also the second moments of the distribution (35) and so, comparing these equations with (43) we find

$$e_1 = \epsilon (E_{11} E_{22} - E_{12}^2)^{1/2} = \epsilon D_1, \quad e_2 = \epsilon (E_{33} E_{44} - E_{34}^2)^{1/2} = \epsilon D_2, \quad (76)$$

$$a_1 = -E_{12}/D_1, \quad b_1 = E_{11}/D_1, \quad g_1 = E_{22}/D_1, \quad (77)$$

$$a_2 = -E_{34}/D_2, \quad b_2 = E_{33}/D_2, \quad g_2 = E_{44}/D_2. \quad (78)$$

The projections (69) are therefore gaussian distributions with rms emittances e_1 and e_2 .

5.5 Evolution of Projection Emittances

The evolution of the x, x' and y, y' projections is given by equations (46–48), (66–68), and (76–78). The emittances of these projections are proportional to the square roots of the determinants $|\mathbf{F}|$ and $|\mathbf{G}|$. Here we derive expressions for these determinants in terms of the initial ellipsoid matrices $\mathbf{F}_0, \mathbf{G}_0$, and \mathbf{C}_0 , and the symplectic transfer matrix \mathbf{T} .

Following Courant and Snyder [1], we define the symplectic conjugate of a two-by-two or four-by-four matrix \mathbf{A} as follows

$$\overline{\mathbf{A}} = -\mathbf{S} \mathbf{A}^\dagger \mathbf{S}, \quad (79)$$

where \mathbf{S} is given by (28). For two-by-two matrices we have

$$\mathbf{A} = \begin{pmatrix} A_{11} & A_{12} \\ A_{21} & A_{22} \end{pmatrix}, \quad \mathbf{S} = \begin{pmatrix} 0 & 1 \\ -1 & 0 \end{pmatrix}, \quad \overline{\mathbf{A}} = \begin{pmatrix} A_{22} & -A_{12} \\ -A_{21} & A_{11} \end{pmatrix}, \quad (80)$$

and

$$\mathbf{A}\overline{\mathbf{A}} = \overline{\mathbf{A}}\mathbf{A} = (A_{11}A_{22} - A_{12}A_{21})\mathbf{I} = |\mathbf{A}|\mathbf{I}, \quad (81)$$

$$\mathbf{A} + \overline{\mathbf{A}} = (A_{11} + A_{22})\mathbf{I} = \text{Tr}(\mathbf{A})\mathbf{I}. \quad (82)$$

For the four-by-four matrix \mathbf{T} we have

$$\mathbf{T}\overline{\mathbf{T}} = \begin{pmatrix} \mathbf{M} & \mathbf{n} \\ \mathbf{m} & \mathbf{N} \end{pmatrix} \begin{pmatrix} \overline{\mathbf{M}} & \overline{\mathbf{m}} \\ \overline{\mathbf{n}} & \overline{\mathbf{N}} \end{pmatrix} = \begin{pmatrix} \mathbf{M}\overline{\mathbf{M}} + \mathbf{n}\overline{\mathbf{n}} & \mathbf{M}\overline{\mathbf{m}} + \mathbf{n}\overline{\mathbf{N}} \\ \mathbf{m}\overline{\mathbf{M}} + \mathbf{N}\overline{\mathbf{n}} & \mathbf{m}\overline{\mathbf{m}} + \mathbf{N}\overline{\mathbf{N}} \end{pmatrix} \quad (83)$$

$$\overline{\mathbf{T}}\mathbf{T} = \begin{pmatrix} \overline{\mathbf{M}} & \overline{\mathbf{m}} \\ \overline{\mathbf{n}} & \overline{\mathbf{N}} \end{pmatrix} \begin{pmatrix} \mathbf{M} & \mathbf{n} \\ \mathbf{m} & \mathbf{N} \end{pmatrix} = \begin{pmatrix} \overline{\mathbf{M}}\mathbf{M} + \overline{\mathbf{m}}\mathbf{m} & \overline{\mathbf{M}}\mathbf{n} + \overline{\mathbf{m}}\mathbf{N} \\ \overline{\mathbf{n}}\mathbf{M} + \overline{\mathbf{N}}\mathbf{m} & \overline{\mathbf{n}}\mathbf{n} + \overline{\mathbf{N}}\mathbf{N} \end{pmatrix}. \quad (84)$$

Now if \mathbf{T} is symplectic, then $\mathbf{T}^\dagger \mathbf{S} \mathbf{T} = \mathbf{S}$, $\mathbf{T}^{-1} \mathbf{S} (\mathbf{T}^\dagger)^{-1} = \mathbf{S}$, $\mathbf{S} = \mathbf{T} \mathbf{S} \mathbf{T}^\dagger$, and therefore

$$\overline{\mathbf{T}}\mathbf{T} = -\mathbf{S}\mathbf{T}^\dagger \mathbf{S} \mathbf{T} = -\mathbf{S}^2 = \mathbf{I}, \quad \mathbf{T}\overline{\mathbf{T}} = -\mathbf{T} \mathbf{S} \mathbf{T}^\dagger = -\mathbf{S}^2 = \mathbf{I}. \quad (85)$$

Using (85) in (83-84) we find

$$|\mathbf{m}| = |\mathbf{n}|, \quad |\mathbf{M}| = |\mathbf{N}|, \quad (86)$$

$$|\mathbf{M}| + |\mathbf{m}| = 1, \quad |\mathbf{N}| + |\mathbf{n}| = 1, \quad (87)$$

$$\overline{\mathbf{M}}\mathbf{n} + \overline{\mathbf{m}}\mathbf{N} = 0, \quad \mathbf{M}\overline{\mathbf{m}} + \mathbf{n}\overline{\mathbf{N}} = 0. \quad (88)$$

Now if

$$\mathbf{E} = \mathbf{T} \mathbf{E}_0 \mathbf{T}^\dagger, \quad (89)$$

then we have

$$\mathbf{E}\overline{\mathbf{E}} = \mathbf{T} \mathbf{E}_0 \mathbf{T}^\dagger \overline{\mathbf{T}}^\dagger \overline{\mathbf{E}}_0 \overline{\mathbf{T}} = \mathbf{T} \mathbf{E}_0 \overline{\mathbf{E}}_0 \overline{\mathbf{T}} \quad (90)$$

and using (44) and (81-82) in (90) we find

$$|\mathbf{F}| + |\mathbf{C}| = |\mathbf{M}||\mathbf{F}_0| + |\mathbf{m}||\mathbf{G}_0| + |\mathbf{C}_0| + \tau \quad (91)$$

$$|\mathbf{G}| + |\mathbf{C}| = |\mathbf{m}||\mathbf{F}_0| + |\mathbf{M}||\mathbf{G}_0| + |\mathbf{C}_0| - \tau \quad (92)$$

$$\tau = \text{Tr}(\mathbf{M}\mathbf{F}_0 \overline{\mathbf{C}}_0^\dagger \overline{\mathbf{n}}) + \text{Tr}(\mathbf{M}\mathbf{C}_0 \overline{\mathbf{G}}_0 \overline{\mathbf{n}}). \quad (93)$$

Thus we have

$$|\mathbf{F}| + |\mathbf{G}| + 2|\mathbf{C}| = |\mathbf{F}_0| + |\mathbf{G}_0| + 2|\mathbf{C}_0|, \quad (94)$$

$$|\mathbf{F}| - |\mathbf{G}| = (1 - 2|\mathbf{m}|)(|\mathbf{F}_0| - |\mathbf{G}_0|) + 2\tau. \quad (95)$$

Using (48), (81–82), and (86–88) we also find

$$|\mathbf{C}| = |\mathbf{M}||\mathbf{m}|(|\mathbf{F}_0| + |\mathbf{G}_0|) - \text{Tr}(\mathbf{M}\mathbf{F}_0\mathbf{M}^\dagger\bar{\mathbf{n}}^\dagger\bar{\mathbf{G}}_0\bar{\mathbf{n}}) + C_1 + C_2 + C_3, \quad (96)$$

where

$$C_1 = (|\mathbf{M}|^2 + |\mathbf{m}|^2)|\mathbf{C}_0| + \text{Tr}(\mathbf{M}\mathbf{C}_0\mathbf{N}^\dagger\bar{\mathbf{m}}^\dagger\bar{\mathbf{C}}_0^\dagger\bar{\mathbf{n}}), \quad (97)$$

$$C_2 = |\mathbf{M}|\text{Tr}(\mathbf{M}\mathbf{C}_0\bar{\mathbf{G}}_0\bar{\mathbf{n}}) + |\mathbf{m}|\text{Tr}(\mathbf{M}\mathbf{F}_0\bar{\mathbf{C}}_0^\dagger\bar{\mathbf{n}}), \quad (98)$$

$$C_3 = \text{Tr}(\mathbf{M}\mathbf{C}_0\mathbf{N}^\dagger\bar{\mathbf{m}}^\dagger\bar{\mathbf{F}}_0\bar{\mathbf{M}}) + \text{Tr}(\mathbf{n}\mathbf{C}_0^\dagger\mathbf{m}^\dagger\bar{\mathbf{N}}^\dagger\bar{\mathbf{G}}_0\bar{\mathbf{n}}). \quad (99)$$

Equations (91–99) give the evolution of the emittances, $\epsilon|\mathbf{F}|^{1/2}$ and $\epsilon|\mathbf{G}|^{1/2}$, of the x, x' and y, y' projections in terms of the partitioned matrices of \mathbf{E}_0 and \mathbf{T} .

For the case in which the initial ellipsoid has no coupling between the x and y planes,

$$\mathbf{C}_0 = \mathbf{0}, \quad (100)$$

and using (91–93) and (96–99) we find

$$|\mathbf{F}| = |\mathbf{M}|^2|\mathbf{F}_0| + |\mathbf{m}|^2|\mathbf{G}_0| + \text{Tr}(\mathbf{M}\mathbf{F}_0\mathbf{M}^\dagger\bar{\mathbf{n}}^\dagger\bar{\mathbf{G}}_0\bar{\mathbf{n}}), \quad (101)$$

$$|\mathbf{G}| = |\mathbf{m}|^2|\mathbf{F}_0| + |\mathbf{M}|^2|\mathbf{G}_0| + \text{Tr}(\mathbf{M}\mathbf{F}_0\mathbf{M}^\dagger\bar{\mathbf{n}}^\dagger\bar{\mathbf{G}}_0\bar{\mathbf{n}}). \quad (102)$$

And since $\tau = 0$ (95) becomes

$$|\mathbf{F}| - |\mathbf{G}| = (1 - 2|\mathbf{m}|)(|\mathbf{F}_0| - |\mathbf{G}_0|). \quad (103)$$

The consequences of this last relation have been worked out by Brown and Servranckx and are discussed in Ref. [2]. Here they also prove that for the case in which there is no coupling ($\mathbf{C}_0 = \mathbf{0}$) in the initial ellipsoid matrix,

$$|\mathbf{F}|^{1/2} \geq (1 - |\mathbf{m}|)|\mathbf{F}_0|^{1/2} + |\mathbf{m}||\mathbf{G}_0|^{1/2}, \quad (104)$$

$$|\mathbf{G}|^{1/2} \geq |\mathbf{m}||\mathbf{F}_0|^{1/2} + (1 - |\mathbf{m}|)|\mathbf{G}_0|^{1/2}, \quad (105)$$

and therefore

$$|\mathbf{F}|^{1/2} + |\mathbf{G}|^{1/2} \geq |\mathbf{F}_0|^{1/2} + |\mathbf{G}_0|^{1/2}. \quad (106)$$

Thus the sum of the emittances of the x, x' and y, y' projections is always greater than or equal to the the sum of the initial uncoupled emittances.

5.6 Transfer Matrix for a Rolled Quadrupole

The transfer matrix for a quadrupole rolled clockwise by angle ϕ is given by

$$\mathbf{q} = \mathbf{R}(-\phi)\mathbf{Q}\mathbf{R}(\phi), \quad (107)$$

where

$$\mathbf{Q} = \begin{pmatrix} \mathbf{M} & \mathbf{0} \\ \mathbf{0} & \mathbf{N} \end{pmatrix}, \quad (108)$$

is the transfer matrix for the unrolled quadrupole, and

$$\mathbf{R}(\phi) = \begin{pmatrix} \mathbf{C} & \mathbf{0} & -\mathbf{S} & \mathbf{0} \\ \mathbf{0} & \mathbf{C} & \mathbf{0} & -\mathbf{S} \\ \mathbf{S} & \mathbf{0} & \mathbf{C} & \mathbf{0} \\ \mathbf{0} & \mathbf{S} & \mathbf{0} & \mathbf{C} \end{pmatrix}, \quad \mathbf{C} = \cos \phi, \quad \mathbf{S} = \sin \phi. \quad (109)$$

Thus we have

$$\mathbf{q} = \begin{pmatrix} \mathbf{C}^2\mathbf{M} + \mathbf{S}^2\mathbf{N} & \mathbf{CS}(\mathbf{N} - \mathbf{M}) \\ \mathbf{CS}(\mathbf{N} - \mathbf{M}) & \mathbf{C}^2\mathbf{N} + \mathbf{S}^2\mathbf{M} \end{pmatrix}. \quad (110)$$

For the case of a skew quadrupole the angle $\phi = 45^\circ$ and (110) becomes

$$\mathbf{q} = \frac{1}{2} \begin{pmatrix} \mathbf{M} + \mathbf{N} & \mathbf{N} - \mathbf{M} \\ \mathbf{N} - \mathbf{M} & \mathbf{M} + \mathbf{N} \end{pmatrix}. \quad (111)$$

For the case of a thin quadrupole we have

$$\mathbf{M} = \begin{pmatrix} 1 & 0 \\ -k & 1 \end{pmatrix}, \quad \mathbf{N} = \begin{pmatrix} 1 & 0 \\ k & 1 \end{pmatrix}, \quad k = 1/f, \quad (112)$$

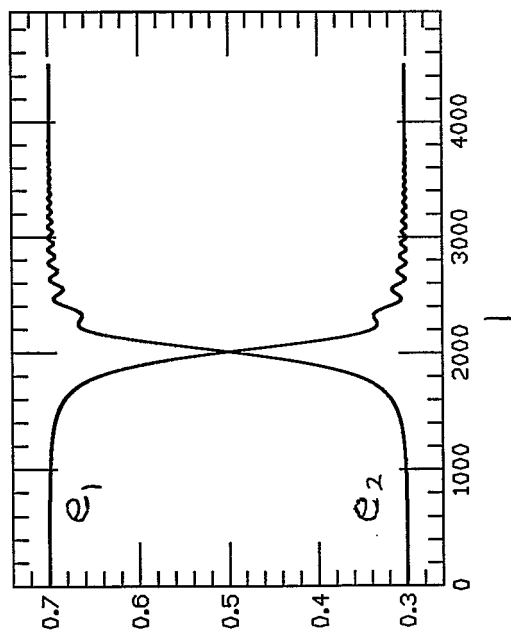
and (111) becomes

$$\mathbf{q} = \begin{pmatrix} \mathbf{I} & \mathbf{k} \\ \mathbf{k} & \mathbf{I} \end{pmatrix}, \quad \mathbf{k} = \begin{pmatrix} 0 & 0 \\ k & 0 \end{pmatrix}. \quad (113)$$

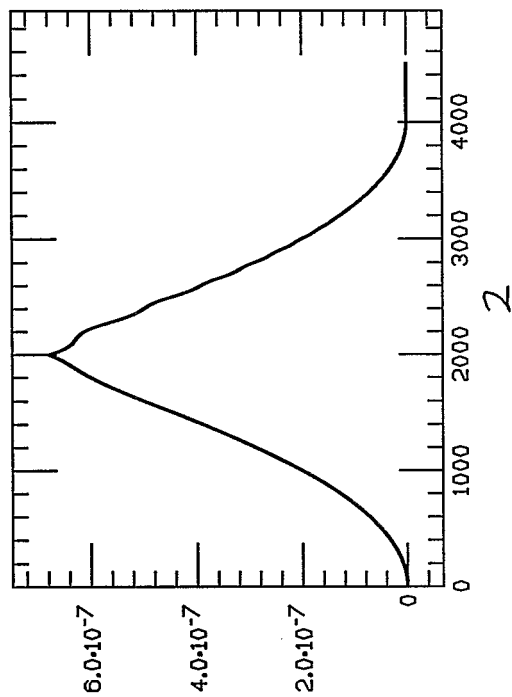
6 References

1. E.D. Courant and H.S. Snyder, *Annals of Physics*, 1958, vol. 3, pp. 1-48.
2. K.L. Brown and R.V. Servranckx, *Particle Accelerators*, 1991, vol. 36, pp. 121-139.

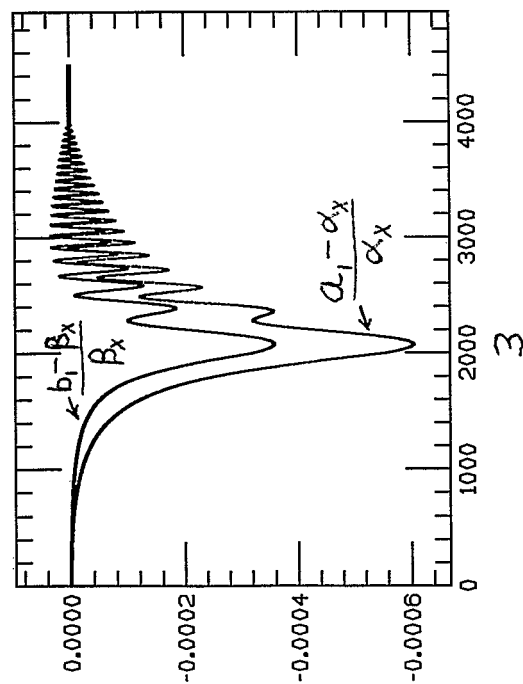
PROJECTION EMITTANCES VS TURN



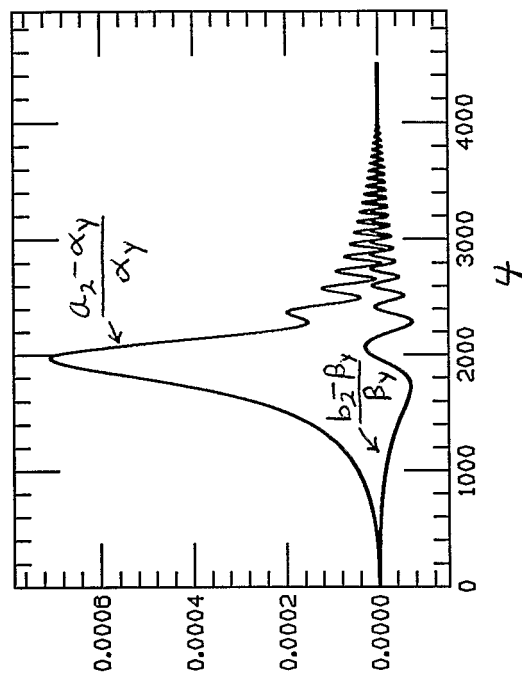
EMITTANCE SUM - 1 VS TURN



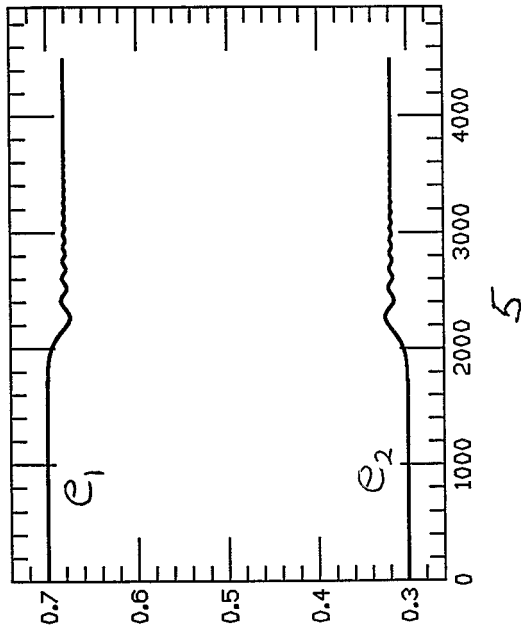
X PROJECTION PARAMETERS VS TURN



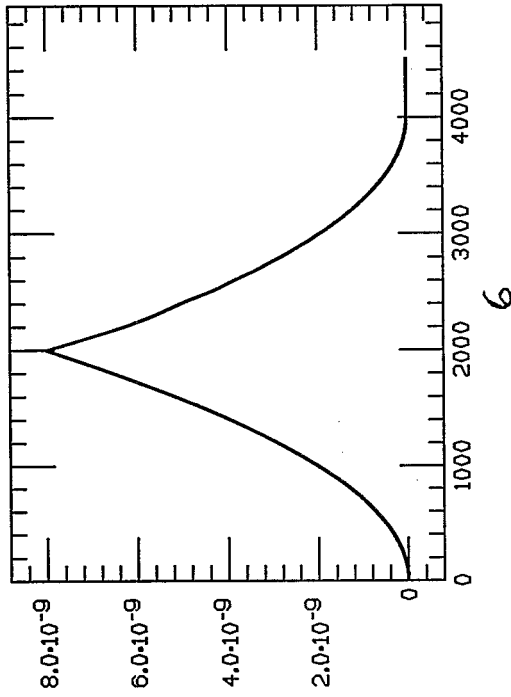
Y PROJECTION PARAMETERS VS TURN



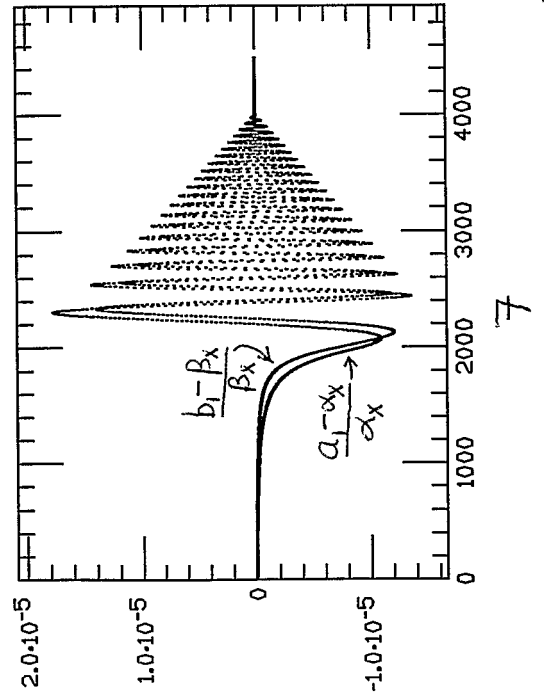
PROJECTION EMITTANCES VS TURN



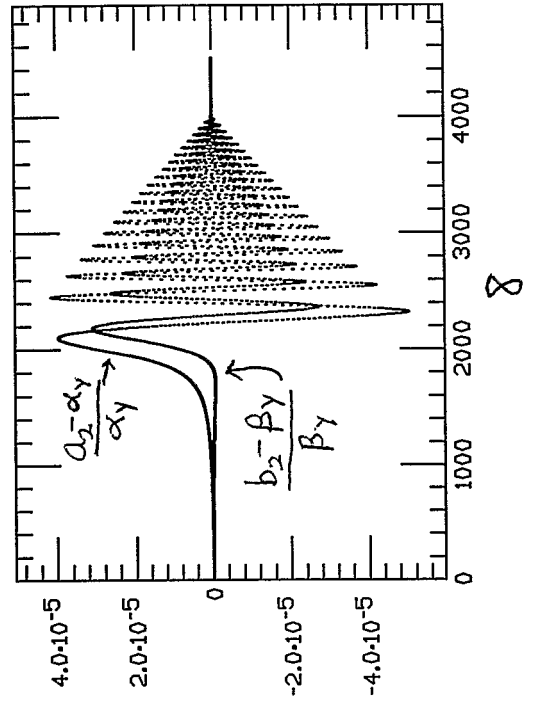
EMITTANCE SUM - 1 VS TURN



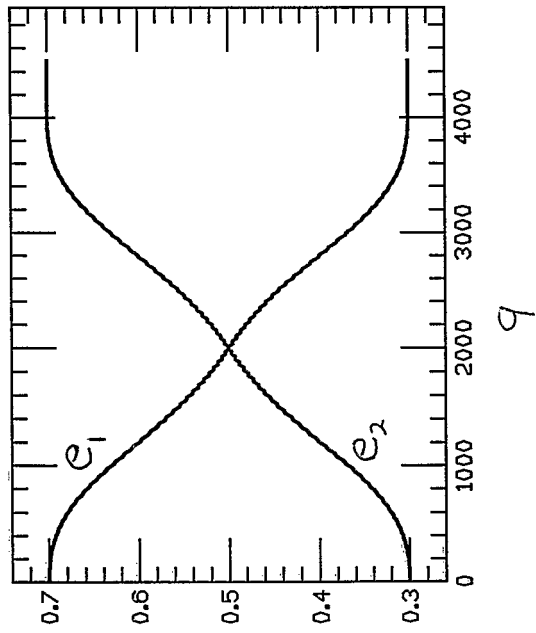
X PROJECTION PARAMETERS VS TURN



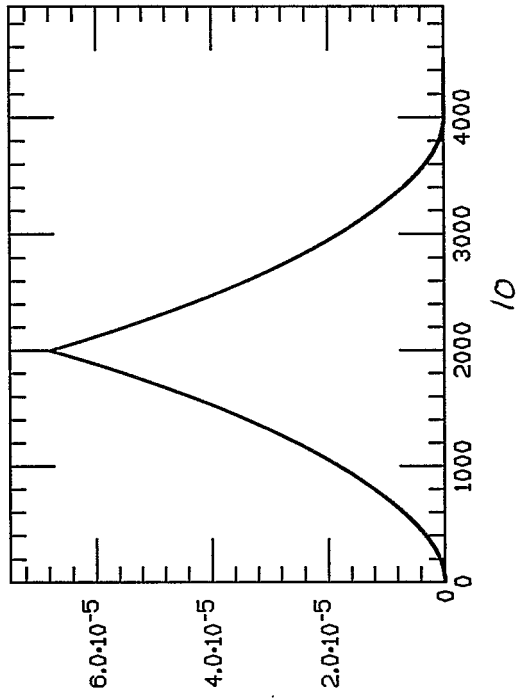
Y PROJECTION PARAMETERS VS TURN



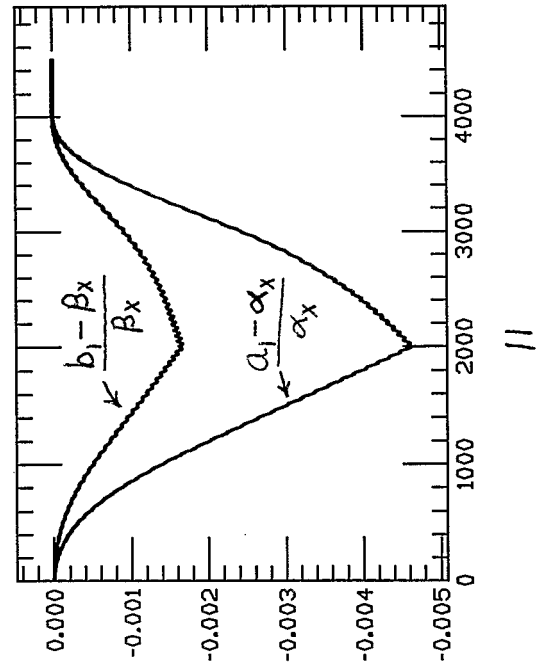
PROJECTION EMITTANCES VS TURN



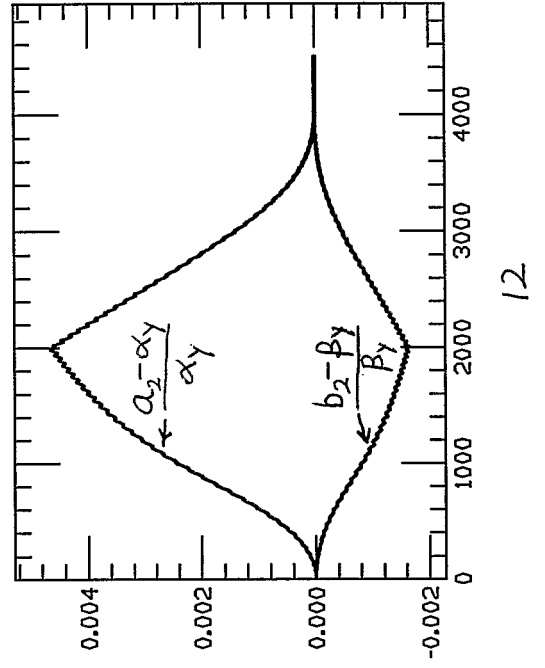
EMITTANCE SUM - 1 VS TURN



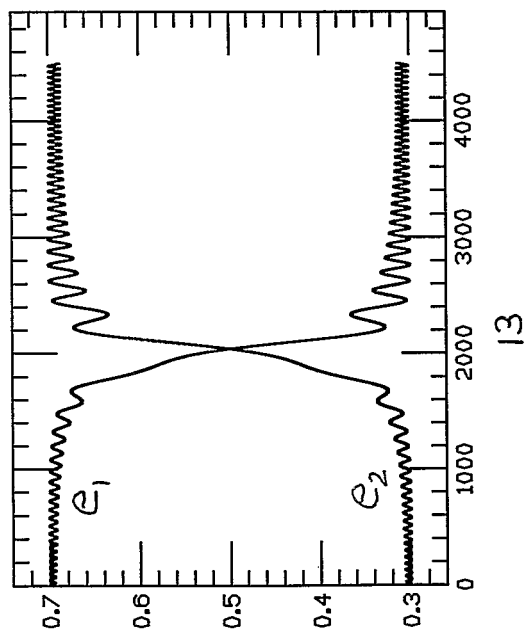
X PROJECTION PARAMETERS VS TURN



Y PROJECTION PARAMETERS VS TURN

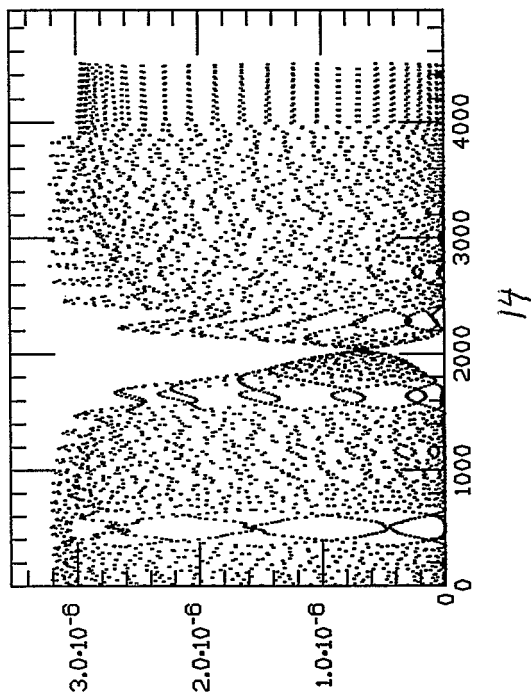


PROJECTION EMITTANCES VS TURN



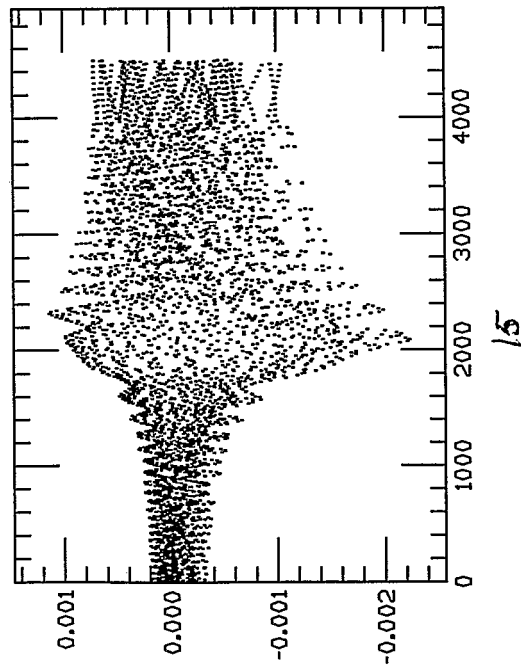
13

EMITTANCE SUM - 1 VS TURN



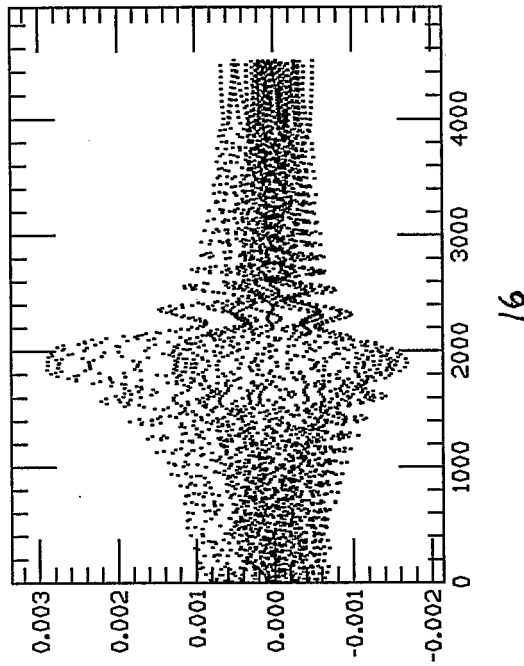
14

X PROJECTION PARAMETERS VS TURN



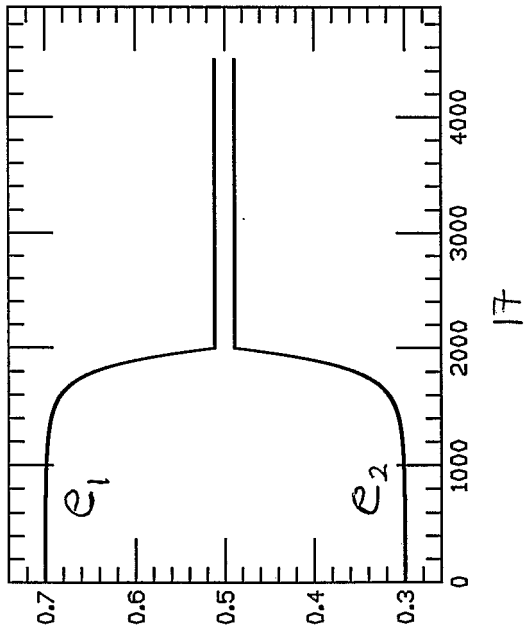
15

Y PROJECTION PARAMETERS VS TURN



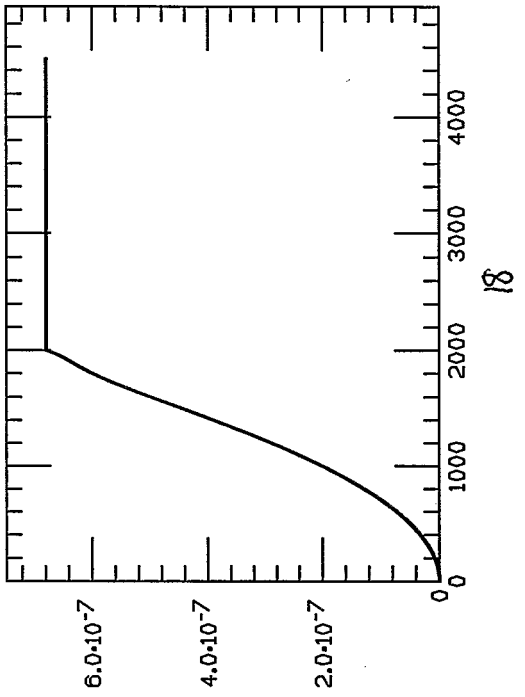
16

PROJECTION EMITTANCES VS TURN



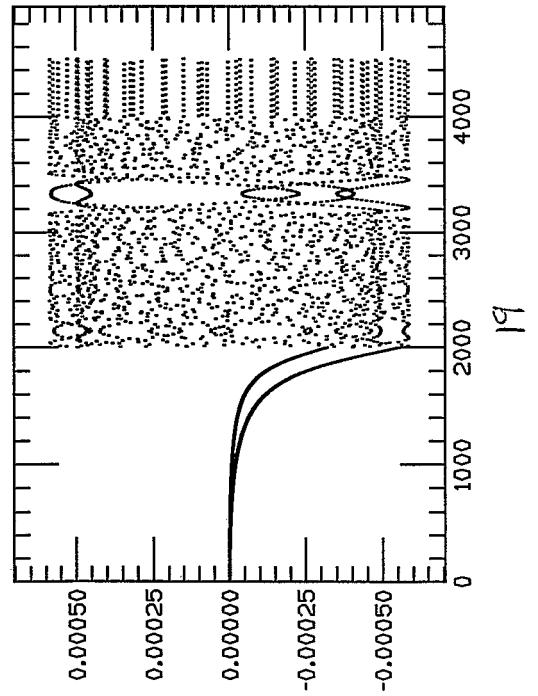
17

EMITTANCE SUM - 1 VS TURN



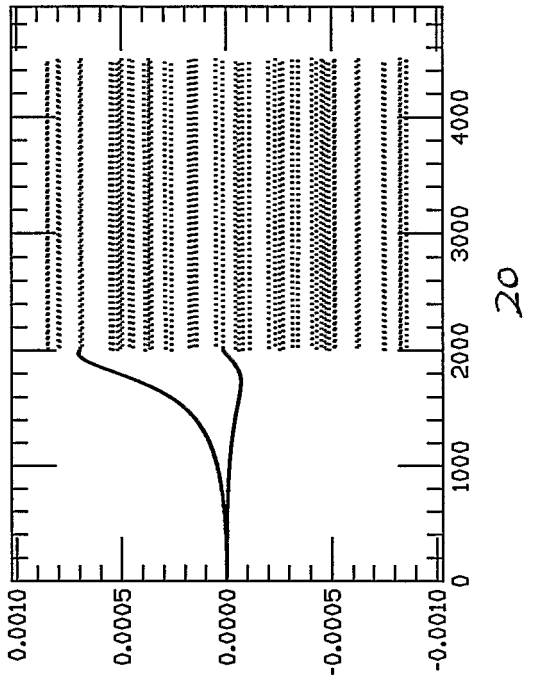
18

X PROJECTION PARAMETERS VS TURN



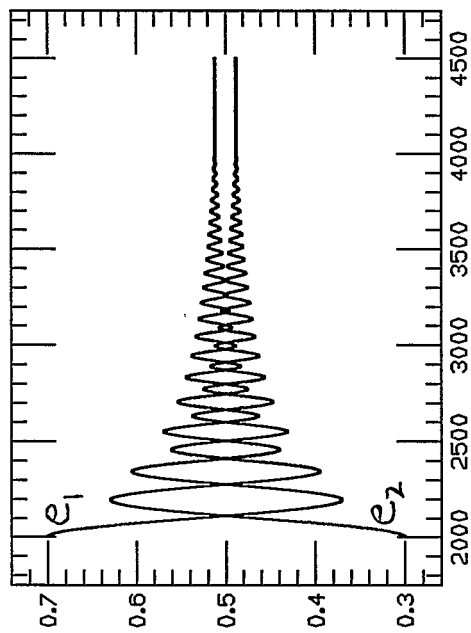
19

Y PROJECTION PARAMETERS VS TURN



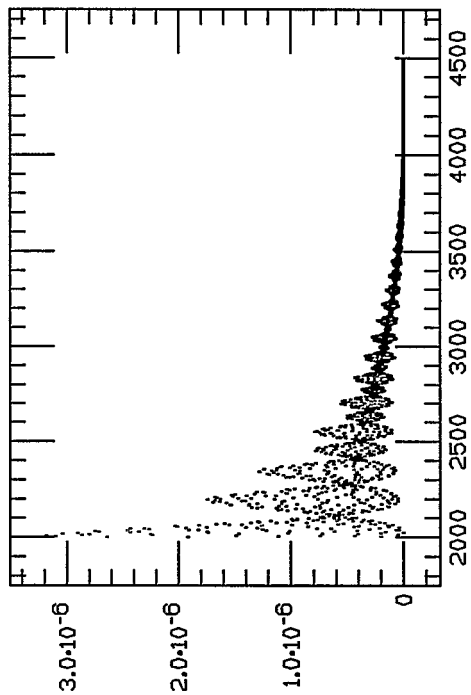
20

PROJECTION EMITTANCES VS TURN



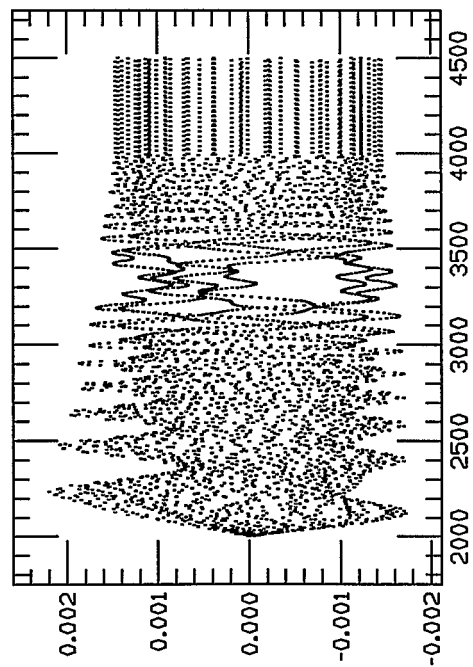
21

EMITTANCE SUM - 1 VS TURN



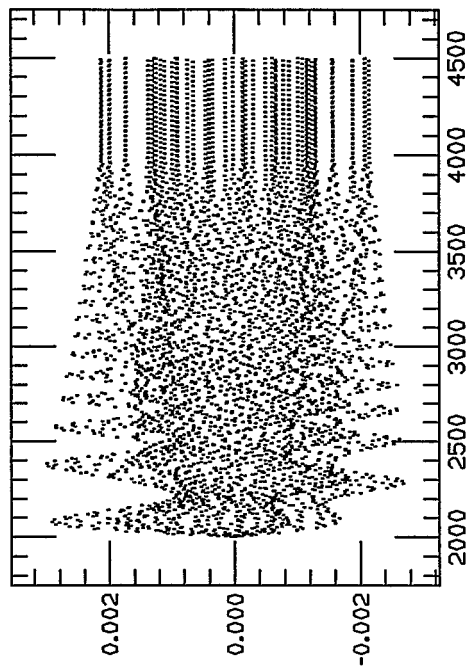
22

X PROJECTION PARAMETERS VS TURN



23

Y PROJECTION PARAMETERS VS TURN



24